Counting Carambolas[*]

Adrian Dumitrescu[†]   Maarten Löffler[‡]   André Schulz[§]   Csaba D. Tóth[¶]

August 13, 2015

Abstract

We give upper and lower bounds on the maximum and minimum number of geometric configurations of various kinds present (as subgraphs) in a triangulation of n points in the plane. Configurations of interest include *convex polygons*, *star-shaped polygons* and *monotone paths*. We also consider related problems for *directed* planar straight-line graphs.

Keywords: convex polygon, star-shaped polygon, monotone path, plane graph, triangulation, counting.

1 Introduction

We consider *plane straight-line graphs* (also referred to as *planar geometric graphs*), where the vertices are points in the plane and the edges are line segments between the corresponding points, no two of which intersect except at common endpoints. According to a classical result of Ajtai et al. [2], the number of plane straight-line graphs on n points in the plane is $O(c^n)$, where c is a large absolute constant.

Problems in extremal graph theory typically ask for the minimum or maximum number of certain subgraphs, e.g., perfect matchings, spanning trees or spanning paths, contained in a graph of a given order. Here we consider extremal problems in plane straight-line graphs, where the classes of subgraphs are defined geometrically (i.e., membership in the class depends on the coordinates of the vertices). For instance, van Kreveld, Löffler, and Pach [13] studied the number of convex polygons (cycles) in geometric triangulations on n points (vertices). They constructed n-vertex triangulations containing $\Omega(1.5028^n)$ convex polygons, and proved that every triangulation on n points in the plane contains $O(1.6181^n)$ convex polygons. Dumitrescu and Tóth [9] subsequently sharpened the upper bound to $O(1.5029^n)$, thereby almost closing the gap between the upper and lower bounds.

In this paper we continue this research direction and investigate the multiplicities of other geometrically defined subgraphs present in a geometric triangulation, such as star-shaped polygons and monotone paths. A *star-shaped* polygon (a.k.a. *carambola*, see Figure 1) is a simple polygon P such that there is a (center) point o in its interior with the property that every ray emanating
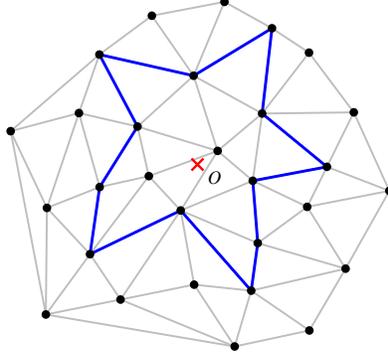

Figure 1: A "carambola" in a triangulation.

from o intersects the boundary of P in exactly one point. As we will see, star-shaped polygons are closely related to monotone paths.

Let $\mathbf{u} \in \mathbb{R}^2 \setminus \{\mathbf{0}\}$ be a nonzero vector (here $\mathbf{0} = (0,0)$). A polygonal path $\xi = (v_1, v_2, \ldots, v_t)$ is *monotone in direction* $\mathbf{u}$, if every line orthogonal to $\mathbf{u}$ intersects ξ in at most one point. Equivalently, a path ξ is *monotone* in direction $\mathbf{u}$, if every directed edge of ξ has a positive scalar product with $\mathbf{u}$, that is, $\langle \overrightarrow{v_i v_{i+1}}, \mathbf{u} \rangle > 0$ for $i = 1, \ldots, t-1$. A special case is an *x-monotone* path, which is monotone in the horizontal direction $\mathbf{u} = (1,0)$. A path $\xi = (v_1, v_2, \ldots, v_t)$ is *monotone* if it is monotone in some direction $\mathbf{u} \in \mathbb{R}^2 \setminus \{\mathbf{0}\}$. Monotone paths are traditionally used in optimization; a classic example is the simplex algorithm for linear programming, which traces a monotone path on the 1-skeleton of a d-dimensional polytope of feasible solutions.

Counting star-shaped polygons and monotone paths in a triangulation T can be reduced to counting directed cycles and paths, respectively, in some orientation of T. Indeed, let o be a center point and orient every edge ab in T as (a,b) iff Δoab is a clockwise triangle. Then the number of star-shaped polygons centered at o equals the number of directed cycles. Similarly, let $\mathbf{u} \in \mathbb{R}^2 \setminus \{\mathbf{0}\}$ be a nonzero vector, and orient every edge ab in T as (a,b) iff $\langle \overrightarrow{ab}, \mathbf{u} \rangle > 0$. Then the number of $\mathbf{u}$-monotone paths in T equals the number of directed paths. To see the role played by the geometric constraints in the definition of these special orientations, we also derive bounds on the maximum and minimum number of directed paths in an oriented n-vertex triangulation.

Our results. In Sections 2 and 3, we derive lower and upper bounds, respectively, on the *maximum* number of subgraphs of a certain kind that a triangulation on n points can contain. Table 1 summarizes known and new results.

Configurations	Lower bound	Upper bound
Convex polygons	$\Omega(1.5028^n)$ [13]	$O(1.5029^n)$ [9]
Star-shaped polygons	$\Omega(1.7003^n)$	$O(n^3 \alpha^n)$
Monotone paths	$\Omega(1.7003^n)$	$O(n \alpha^n)$
Directed simple paths	$\Omega(\alpha^n)$	$O(n^2 3^n)$

Table 1: Bounds for the maximum number of configurations in an n-vertex plane graph. Results in row 1 are included for comparison; the bounds in rows 2-4 are proved in the paper. Row 4 concerns directed graphs. Note: $\alpha = 1.8392\ldots$ is the unique real root of the cubic equation $x^3 - x^2 - x - 1 = 0$.

In Section 4, we study the *minimum* number of configurations that a triangulation on n vertices can contain. Our asymptotic bounds are summarized in Table 2; more precise estimates are available

in the respective section.

Configurations	Lower bound	Upper bound
Convex polygons	$\Omega(n)$	$O(n)$
Star-shaped polygons	$\Omega(n)$	$O(n^2)$
Monotone paths	$\Omega(n^2)$	$O(n^{3.17})$
Directed paths	$\Omega(n)$	$O(n)$

Table 2: Bounds for the minimum number of configurations in a triangulation with n vertices. Row 4 concerns directed triangulations.

Related work. Previous research studied the maximum number of cycles and spanning trees in triangulations with n vertices. Since cycles and spanning trees, in general, have no geometric attributes, upper bounds on these numbers hold for all edge-maximal planar graph, i.e., combinatorial triangulations. Buchin et al. [4] showed that every triangulation with n vertices contains $O(2.8928^n)$ simple cycles, and there are triangulations that contain $\Omega(2.4262^n)$ simple cycles and $\Omega(2.0845^n)$ Hamiltonian cycles. Buchin and Schulz [5] proved that every n-vertex triangulation contains $O(5.2852^n)$ spanning trees. These techniques are instrumental for bounding the total number of noncrossing Hamiltonian cycles and spanning trees that n points in the plane admit [10, 16]. Some recent lower bounds on these numbers appear in [7]; see also [1, 8, 10] and the references therein for other related results.

2 Lower bounds on the maximum number of subgraphs

2.1 Monotone paths

We construct plane straight-line graphs on n vertices that contain $\Omega(1.7003^n)$ x-monotone paths; see Figure 2. Thus by orienting all edges from left to right, we obtain a directed plane straight-line graph that contains $\Omega(1.7003^n)$ directed paths. The same construction yields lower bounds for a few related subgraphs. By arranging three copies of this graph around the origin in a cyclic fashion as shown in Figure 5, we obtain a plane straight-line graph that contains $\Omega(1.7003^n)$ star-shaped polygons. By connecting the leftmost and rightmost vertices by two extra edges to a common vertex, we obtain a plane straight-line graph that contains $\Omega(1.7003^n)$ monotone polygons, (defined as usual; see e.g., [3, p. 49]).
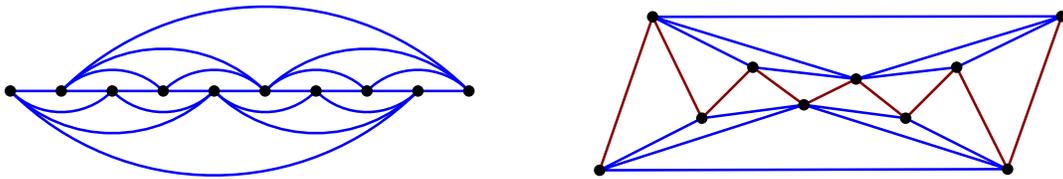

Figure 2: Left: a graph on $n = 2^\ell + 2$ vertices (here $\ell = 3$), that contains $\Omega(1.7003^n)$ monotone paths, for n sufficiently large. Right: a straight-line embedding of the same graph where the points lie alternately on two circular arcs, while preserving x-monotonicity.

Let $n = 2^\ell + 2$ for an integer $\ell \in \mathbb{N}$. We define a plane graph G on n vertices $V = \{v_1, \ldots, v_n\}$: it consists of a path $\pi = (v_1, \ldots, v_n)$ and two balanced binary triangulations of the vertices $\{v_1, \ldots, v_{n-1}\}$ and $\{v_2, \ldots, v_n\}$, respectively, one on each side of the path; see Figure 2 (left).

Specifically, G contains an edge (v_i, v_{i+2^k}), for $1 \le i \le n - 2^k$, if and only if $i - 1$ or $i - 2$ is a multiple of 2^k. A straight-line embedding is shown in Figure 2 (right), where the odd and respectively the even vertices lie on two convex polygonal chains with opposite orientations.

Theorem 1. *The graph G described in the preceding paragraph has $\Omega(1.7003^n)$ x-monotone paths.*

Proof. We count the number of x-monotone paths in a sequence of subgraphs of G. Let G_0 be the path $\pi = (v_1, \dots, v_n)$; and we recursively define G_k from G_{k-1} by adding the edges (v_i, v_{i+2^k}) for $i = j2^k + 1$ and $i = j2^k + 2$ for $j = 0, 1, \dots, 2^{\ell-k} - 1$. The final graph is G_ℓ. Denote by $p_k(v_i)$ the number of x-monotone paths in G_k that end at vertex v_i. Since every monotone path can be extended to the rightmost vertex v_n, the number of maximal (with respect to containment) monotone paths in G_k is $p_k(v_n)$.

We establish the following recurrence relations for $p_k(v_i)$. The initial values are $p_k(v_1) = p_k(v_2) = 1$ and $p_k(v_3) = 2$ for all $k = 0, \dots, \ell$. For $k = 1$ and $i \ge 3$, we have $p_1(v_i) = p_1(v_{i-1}) + p_1(v_{i-2})$, therefore $p_1(v_i) = F_i$, where F_i is the ith Fibonacci number. It is well known that $F_i = \Theta(\phi^n)$, where $\phi = (1 + \sqrt{5})/2 = 1.6180\dots$, so $p_1(v_n) = \Theta(\phi^n)$.

The recurrence for $p_k(v_i)$, $k \ge 2$, is more nuanced, due to the asymmetry between the triangulations on the two sides of the path π. We partition the edges of graph G_k into groups, each induced by $2^{k-1} + 2$ consecutive vertices (with respect to π), such that every two consecutive groups share two vertices. Let a_i denote the first vertex of group i, and let b_i be the second vertex of group i. Let the edge (a_i, b_i) belong to group i but not to group $i - 1$. We count the number of ways one can route an x-monotone path through a group. A path through group i starts at either a_i or b_i, and ends at either a_{i+1} or b_{i+1}. Thus, it is enough to keep track of four different types of paths. We record the number of paths from a_i or b_i to a_{i+1} or b_{i+1} in a 2×2 matrix M_k, such that

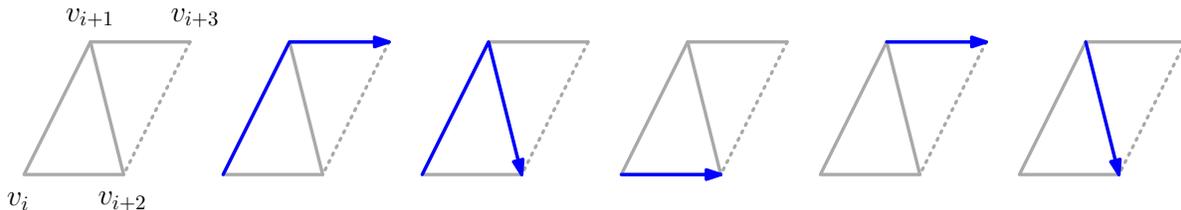$$M_k \cdot (p_k(a_i), p_k(b_i))^T = (p_k(a_{i+1}), p_k(b_{i+1}))^T.$$

Figure 3: The five possible x-monotone paths in the group of G_2.

Once the matrix M_k is known, we can compute the number of paths by $(p(v_{n-1}), p(v_n))^T = M_k^{(n-2)/2^{k-1}} \cdot (1,1)^T$. By the Perron–Frobenius Theorem [11], $\lim_{q \to \infty} M_k^q / \lambda^q = A$, for some matrix A, and for λ being the largest eigenvalue of M_k. Hence, we have $\lim_{n \to \infty} p_k(v_n) = \Theta(\lambda^{n/2^{k-1}})$ maximal x-monotone paths in G_k.
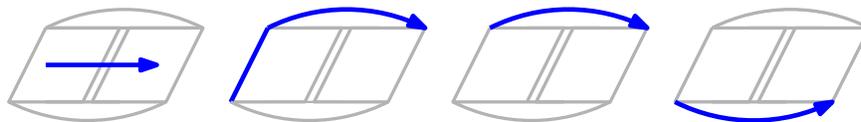

Figure 4: Schematic drawing of the paths counted by M_k.

We now show how to compute the matrices M_k by induction on k. The matrix M_2 can be easily obtained by hand (see Figure 3). For computing M_k, $k \ge 3$, consider an arbitrary group i

of size $2^{k-1} + 2$ in G_k. This group is composed of two consecutive groups of G_{k-1} that share two common vertices, say a_j and b_j, and two additional edges $a_i a_{i+1}$ and $b_i b_{i+1}$. We distinguish two types of paths in group i of G_k: (1) Paths that use only the edges in G_{k-1}. Every such path is the concatenation of two paths, from two consecutive groups of G_{k-1}, with a common endpoint a_j or b_j. The number of these paths from a_i or b_i to a_{i+1} or b_{i+1} is precisely M_{k-1}^2. (2) The paths that use $a_i a_{i+1}$ or $b_i b_{i+1}$. Since edge $a_i b_i$ is part of group i, but edge $a_{i+1} b_{i+1}$ is not, the only possible paths are (a_i, a_{i+1}), (a_i, b_i, b_{i+1}), and (b_i, b_{i+1}); see Figure 4. Therefore, we can compute the matrices M_k iteratively as follows:

$$M_2 := \begin{pmatrix} 2 & 1 \\ 1 & 1 \end{pmatrix}, \text{ and } M_k := M_{k-1}^2 + \begin{pmatrix} 1 & 0 \\ 1 & 1 \end{pmatrix}.$$

k	2	3	4	5	6
$\lambda^{1/2^{k-1}}$	1.61803	1.69605	1.70034	1.70037	1.70037

Table 3: The asymptotic growth of the number of x-monotone paths in the graphs G_k. Already for $k = 4$ there are $\Omega(1.7003^n)$ monotone paths.

Table 3 shows the values $\lambda^{1/2^{k-1}}$ for $k = 2, \ldots, 6$. Note that when going from $k = 5$ to $k = 6$, there is no change in $\lambda^{1/2^{k-1}}$ up to 8 digits after the decimal point. The precise value of λ for $k = 5$ equals $\lambda = \frac{1}{2}(4885 + 9\sqrt{294153})$. $\qquad\square$

2.2 Star-shaped polygons

Use a projective transformation of the plane straight-line graph in Figure 2 in which the point at infinity in direction $(0,1)$ moves to the center o of the equilateral triangle in Figure 5. Use three copies of the resulting graph; the monotone order becomes a cyclic order with respect to the center o. The plane straight-line graph in Figure 5 has $\Omega(1.7003^n)$ star shaped polygons, obtained by concatenating the images of any three maximal monotone paths, one in each copy.
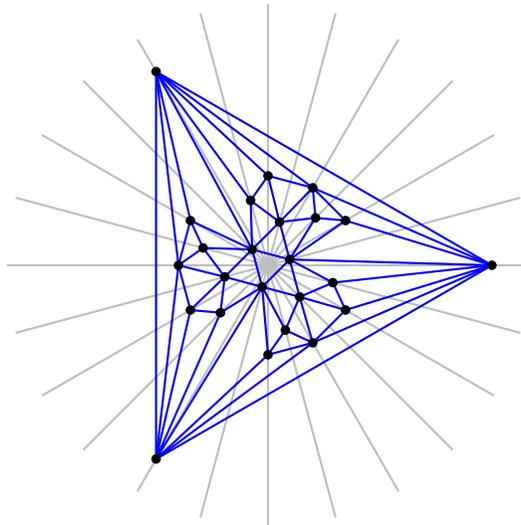

Figure 5: Cyclic embedding of 3 copies of the graph in Figure 2. The monotone order becomes a cyclic order.

2.3 Directed plane graphs

We construct n-vertex directed plane straight-line graphs that contain $\Omega(1.8392^n)$ directed paths; Figure 6 shows the directed graph and Figure 7 shows a planar embedding. It is worth noting that the directed paths, however, cannot be extended to a cycle because in a planar embedding the start and end vertex are not in the same face. Similarly, most of the directed paths are not monotone in any direction in a planar embedding.
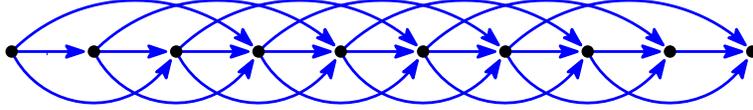

Figure 6: There are $\Theta(\alpha^n)$ directed paths in this graph. A plane embedding of the graph is depicted in Figure 7. Note: $\alpha = 1.8392\ldots$ is the unique real root of the cubic equation $x^3 - x^2 - x - 1 = 0$.
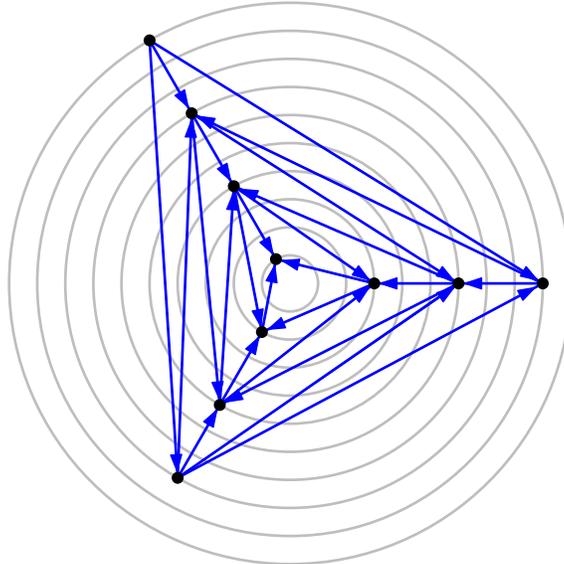

Figure 7: A plane embedding of the graph in Figure 6. The edges are directed from outer circles to inner circles.

Denoting by $T(i)$ the number of directed paths ending at vertex v_i, we have $T(1) = T(2) = 1$, $T(3) = 2$, and a linear recurrence relation

$$T(i) = T(i-1) + T(i-2) + T(i-3), \quad \text{for } i \geq 4.$$

The recurrence solves to $T(i) = \Theta(\alpha^i)$, where $\alpha = 1.8392\ldots$ is the unique real root of the cubic equation $x^3 - x^2 - x - 1 = 0$. Therefore the total number of directed paths, starting at any vertex, is $\Theta(\alpha^n)$.

3 Upper bounds on the maximum number of subgraphs

3.1 Monotone paths

We start with x-monotone paths in a plane straight-line graph. We prove the upper bound for a broader class of graphs, since some of the operations in our argument may not preserve straight-

line edges. A *plane monotone graph* is a graph embedded in the plane such that every edge is an x-monotone Jordan arc.

Let $n \in \mathbb{N}$, $n \geq 3$, and let $G = (V, E)$ be a plane monotone graph with $|V| = n$ vertices that maximizes the number of x-monotone paths. We may assume that (i) the vertices have distinct x-coordinates (otherwise we can perturb the vertices without decreasing the number of x-monotone paths) and (ii) the vertices lie on the x-axis (by applying a homeomorphism that affects the y-coordinates). We may also assume that G is fully triangulated (i.e., it is an edge-maximal planar graph), since adding x-monotone edges can only increase the number of x-monotone paths [15].

Label the vertices in V as $v_1, v_2, \ldots, v_n$, sorted by their x-coordinates. Orient each edge $\{v_i, v_j\} \in E$ from left to right, i.e., from v_i to v_j if $i < j$. Define the *length* of an edge $\overline{v_i v_j} \in E$ by $\text{len}(\overline{v_i v_j}) = |i - j| = j - i$.

Consider an edge $\overline{v_i v_j} \in E$ that is not on the boundary of the outer face. There are two bounded faces incident to $\overline{v_i v_j}$, and at least two other vertices v_k and v_l that are adjacent to both v_i and v_j. Suppose that $i < k, l < j$, and without loss of generality, that $k < l$ (i.e., $i < k < l < j$). The *flip operation* for the edge $\overline{v_i v_j}$ replaces $\overline{v_i v_j}$ by the edge $\overline{v_k v_l}$; note that this operation preserves planarity but may introduce curved edges.

Lemma 1. *If $i < k < l < j$ as described above, then flipping $\overline{v_i v_j}$ to $\overline{v_k v_l}$ produces a plane monotone graph G' with at least as many x-monotone paths as G (see Figure 8.)*
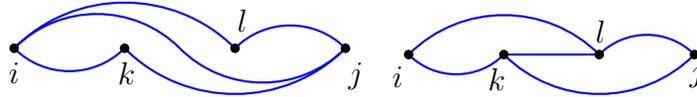

Figure 8: The flip operation.

Proof. The deletion of edge $\overline{v_i v_j}$ from G creates a quadrilateral face (v_i, v_k, v_j, v_l). Since $i < k < l < j$, the new edge $\overline{v_k v_l}$ can be embedded in the interior of this face as an x-monotone Jordan arc.

Every x-monotone path in G that does not contain $\overline{v_i v_j}$ is present in G'. Define an injective map from the set of x-monotone paths that traverse $\overline{v_i v_j}$ in G into the set of x-monotone paths that traverse $\overline{v_k v_l}$ in G'. To every x-monotone path ξ that traverses $\overline{v_i v_j}$ in G, map an x-monotone path ξ' obtained by replacing edge $\overline{v_i v_j}$ with the path (v_i, v_k, v_l, v_j) in G'. It follows that G' contains at least as many x-monotone paths as G. $\square$

Note that the flip operation described in Lemma 1 decreases the total length of the edges $\sum_{e \in E} \text{len}(e)$. We may now assume that among all n-vertex plane monotone graphs with the maximum number of x-monotone paths, G has minimal total edge length. Thus Lemma 1 is inapplicable and we have the following.

Lemma 2. *For every interior edge $\overline{v_i v_j} \in E$, with $i < j$, there is a triangular face (v_i, v_j, v_k) such that either $k < i < j$ or $i < j < k$.*

We show next that G contains an x-monotone Hamiltonian path.

Lemma 3. *All edges $\overline{v_i v_{i+1}}$ are present in G.*

Proof. Suppose, to the contrary, that there are two nonadjacent vertices v_i and v_{i+1}. Since G is a triangulation, $v_i v_{i+1}$ is not a boundary segment, and so there exists an edge that crosses the line segment $v_i v_{i+1}$. Let $\overline{v_j v_k}$, $j < k$, be a longest edge with this property. Since the edge $\overline{v_j v_k}$ is

7

x-monotone, we have $j < i < i+1 < k$. The edge $\overline{v_j v_k}$ is not adjacent to the outer face, since it crosses the segment $v_i v_{i+1}$ between two vertices. Since edge $\overline{v_j v_k}$ is interior, by Lemma 2, there is a triangular face (v_j, v_k, v_l) such that either $l < j < k$ or $j < k < l$. Without loss of generality, assume that $j < k < l$. Since there is no vertex in the interior of the face (v_j, v_k, v_l), the boundary of the face has to cross the segment $v_i v_{i+1}$ twice: that is, $\overline{v_j v_l}$ crosses the segment $v_i v_{i+1}$. Since $j < k < l$, we have $l - j > k - j$, thus $\overline{v_j v_l}$ is longer than $\overline{v_j v_k}$, in contradiction to the assumption that $\overline{v_j v_k}$ is a longest edge crossing $v_i v_{i+1}$. $\qquad\square$

For every pair $i < j$, let V_{ij} denote the set of consecutive vertices $v_i, v_{i+1}, \ldots, v_j$, and let $G_{ij} = (V_{ij}, E_{ij})$ be the subgraph of G induced by V_{ij}. Since G is planar, we know that $|E| \leq 3|V| - 6$, and furthermore, that $|E_{ij}| \leq 3|V_{ij}| - 6$ for all subgraphs induced by groups of 3 or more consecutive vertices.

In the remainder of the proof we will apply a sequence of shift operations on G (defined subsequently) that may create multiple edges and edge crossings. Hence, we consider G as an abstract multigraph. However, the operations will maintain the invariant that $|E_{ij}| \leq 3|V_{ij}| - 6$ whenever $|V_{ij}| \geq 3$.

Let $i < j < k$ be a triple of indices such that $\overline{v_i v_j}, \overline{v_i v_k} \in E$. The operation shift$(i, j, k)$ removes the edge $\overline{v_i v_k}$ from E, and inserts the edge $\overline{v_j v_k}$ into E (see Figure 9). Note that the new edge may already have been present, in this case we insert a new copy of this edge (i.e., we increment its multiplicity by one).
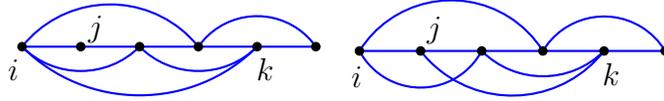

Figure 9: The operation shift(i, j, k).

Lemma 4. *The operation shift(i, j, k) does not decrease the number of x-monotone paths in G.*

Proof. Clearly, any path that used $\overline{v_i v_k}$ can be replaced by a path that uses $\overline{v_i v_j}$ and (the new copy of) $\overline{v_j v_k}$. $\qquad\square$

Now, we apply the following algorithm to the input graph G. We process the vertices from left to right, and whenever we encounter a vertex v_i with outdegree 4 or higher, we identify the smallest index j such that v_i has an edge to v_j and the largest index k such that v_i has an edge to v_k; and then apply shift(i, j, k). We repeat until there are no more vertices with outdegree larger than 3.

Lemma 5. *The algorithm terminates and maintains the following two invariants:*

(I1) *All edges $\overline{v_i v_{i+1}}$ are present in G with multiplicity one.*
(I2) *$|E_{ij}| \leq 3|V_{ij}| - 6$ for all subgraphs induced by V_{ij}, $i < j$.*

Proof. Initially, invariant (I1) holds by Lemma 3, and (I2) by planarity. Edges between consecutive vertices are neither removed nor added in the course of the algorithm, consequently (I1) is maintained. To show that (I2) is maintained, suppose the contrary, that there is an operation that increases the number of edges of an induced subgraph G' above the threshold. Let shift(i, j, k) be the first such operation. Since the only new edge is $\overline{v_j v_k}$, the subgraph G' must contain both v_j and v_k; and it cannot contain v_i since the only edge removed is $\overline{v_i v_k}$. Recall that v_j was the leftmost vertex that v_i is adjacent to; and by invariant (I1), we know $j = i + 1$. Therefore, $G' = G_{jk'}$ for some $k' \geq k$, and we have $|E_{jk'}| \geq 3|V_{jk'}| - 5$ after the shift. Since v_k was the rightmost vertex

8

adjacent to v_i before the shift, all outgoing edges of v_i went to vertices in $V_{jk'}$. The outdegree of v_i was at least 4 before the shift, hence $G_{ik'}$ had at least $3(|V_{ik'}| - 1) - 5 + 4 = 3|V_{ik'}| - 4 > 3|V_{ik'}| - 6$ edges, which is a contradiction. $\qquad\square$

Now, after executing the algorithm, we are left with a multigraph where the outdegree of every vertex is at most 3, and no subgraph induced by $|V_{i,j}| \geq 3$ consecutive vertices has more than $3|V_{ij}| - 6$ edges. This, combined with invariant (I1), implies that the multiplicity of any edge $\overline{v_i v_{i+2}}$ is at most one. Thus, for every vertex v_i, the (at most) three outgoing edges go to vertices at distance at least 1, 2, and 3, respectively, from v_i. Denoting by $T(i)$ the number of x-monotone paths that start at v_{n-i+1}, we arrive at the recurrence

$$T(i) \leq T(i-1) + T(i-2) + T(i-3), \quad \text{for } i \geq 4,$$

with initial values $T(1) = T(2) = 1$ and $T(3) = 2$. The recurrence solves to $T(n) = O(\alpha^n)$ where $\alpha = 1.8392\ldots$ is the unique real root of the cubic equation $x^3 - x^2 - x - 1 = 0$. Therefore, every plane monotone graph on n vertices admits $O(\alpha^n)$ x-monotone paths. In particular, every plane straight-line graph on n vertices admits $O(\alpha^n)$ x-monotone paths.

Since the edges of an n-vertex planar straight-line graph have at most $3n - 6 = O(n)$ distinct directions, the number of monotone paths (over all directions) is bounded from above by $O(n\alpha^n)$. We summarize our results as follows.

Theorem 2. *For every $n \in \mathbb{N}$, every triangulation on n points contains $O(\alpha^n)$ x-monotone paths and $O(n\alpha^n)$ monotone paths, where $\alpha = 1.8392\ldots$ is the unique real root of $x^3 - x^2 - x - 1 = 0$.*

3.2 Star-shaped polygons

Given a plane straight-line graph G on n vertices, the lines passing through the $O(n)$ edges of G induce a line arrangement with $O(n^2)$ faces. Choose a face f of the arrangement, and a vertex v of G. We show that G contains $O(\alpha^n)$ star-shaped polygons incident to vertex v and with a star center lying in f. Indeed, pick an arbitrary point $o \in f$. Each edge of G is oriented either clockwise or counterclockwise with respect to o (with the same orientation for any $o \in f$). Order the vertices of G by a rotational sweep around o starting from the ray $\overrightarrow{ov}$. Let $G_{f,v}$ be the graph obtained from G by deleting all edges that cross the ray $\overrightarrow{ov}$. We can repeat our previous argument for monotone paths for $G_{f,v}$, replacing the x-monotone order by the rotational sweep order about o, and conclude that G admits $O(\alpha^n)$ star-shaped polygons incident to vertex v and with the star center in f. Summing over the $O(n)$ choices for v and the $O(n^2)$ choices for f, we deduce that G admits $O(n^3 \alpha^n)$ star-shaped polygons.

3.3 Directed simple paths

Let $G = (V, E)$ be a directed planar graph. Denote by $\deg^+(v)$ the outdegree of vertex $v \in V$; let $V^+ = \{v_1, \ldots, v_\ell\}$ be the set of vertices with outdegree at least 1, where $1 \leq \ell \leq n$. We show that for every $v \in V^+$, there are $O(3^n)$ maximal (with respect to containment) directed simple paths in G starting from v. Each maximal directed simple path can be encoded in an ℓ-dimensional vector that contains the outgoing edge of each vertex $v \in V^+$ in the path (and an arbitrary outgoing edge if $v \in V^+$ is not part of the path). The number of such vectors is

$$\prod_{i=1}^{\ell} \deg^+(v_i) \leq \left(\frac{1}{\ell} \sum_{i=1}^{\ell} \deg^+(v_i) \right)^\ell < \left(\frac{3n}{\ell} \right)^\ell \leq 3^n,$$

9

where we have used the geometric-arithmetic mean inequality, and the fact that by Euler's formula $\sum_{i=1}^{\ell} \deg^+(v_i) \leq 3n - 6 < 3n$. We then have maximized the function $x \to (3n/x)^x$ over the interval $1 \leq x \leq n$. Since there are $O(n)$ choices for the starting vertex $v \in V^+$, and a maximal simple path contains $O(n)$ nonmaximal paths starting from the same vertex, the total number of simple paths is $O(n^2 3^n)$.

4 Bounds on the minimum number of subgraphs

In this section, we explore the *minimum* number of geometric subgraphs of a certain kind that a triangulation on n points in the plane can have. We start with some easier results concerning convex polygons, star-shaped polygons, and directed paths (in the next three subsections). The most difficult result (concerning monotone paths) is deferred to the last subsection.

4.1 Convex polygons

Every n-vertex triangulation has at least $n - 2$ triangular faces, hence $n - 2$ is a trivial lower bound for the number of convex polygons. Hurtado, Noy and Urrutia [12] proved that every triangulation contains at least $\lceil n/2 \rceil$ pairs of triangles whose union is convex, and this bound is the best possible. Consequently, every triangulation contains at least $3n/2 - O(1)$ convex polygons, each bounding one or two faces. The n-vertex triangulations in Figure 10 (left) contains $4n - O(1)$ convex polygons, and so this bound is the best possible apart from constant factors. The triangulation consists of the join of two paths, $P_2 * P_{n-2}$, where the path P_{n-2} is realized as a monotone zig-zag path. Every convex polygon is either a triangle or the union of two adjacent triangles that share a flippable edge [12].
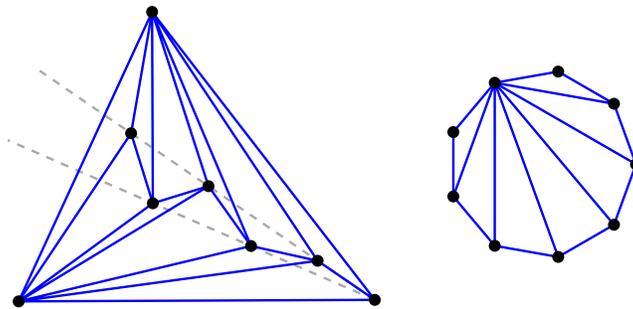

Figure 10: There are $\Theta(n)$ convex polygons and x-monotone paths in the triangulation on the left; it contains $\Theta(n^4)$ star-shaped polygons and monotone paths. There are $\Theta(n^2)$ star-shaped polygons and $\Theta(n^4)$ monotone paths in the triangulation on the right.

4.2 Star-shaped polygons

Every convex polygon is star-shaped, and so the $3n/2 - O(1)$ lower bound on the number of convex polygons in a triangulation on n points (from the previous paragraph) also holds for star-shaped polygons. The following averaging argument yields an improved lower bound.

Consider a triangulation $T = (V, E)$ on n points, k of which are in the interior of the convex hull of V. Then T has $n + k - 2$ bounded (triangular) faces, $2n + k - 3$ edges, $n + 2k - 3$ of which are interior edges. Consequently, the average vertex degree in T is $4 + 2(k - 3)/n$. For each vertex $v \in V$, every sequence of consecutive faces incident to v forms a star-shaped polygon. The number

of such sequences is $2\binom{\deg(v)}{2} + 1$ for interior vertices and $\binom{\deg(v)}{2}$ for boundary vertices. However, summation over all $v \in V$ counts every triangular face three times, and every quadrilateral formed by a pair of adjacent faces twice. Consequently, the number of star-shaped polygons formed by the union of faces with a common vertex is at least

$$\sum_{v \in V} \binom{\deg(v)}{2} + k - 2(n + k - 2) - (n + 2k - 3)$$

$$\geq n \binom{4 + 2(k-3)/n}{2} - 3n - 3k + 7$$

$$\geq \frac{n}{2} \cdot \left(4 + \frac{2(k-3)}{n}\right)\left(3 + \frac{2(k-3)}{n}\right) - 3n - 3k + 7$$

$$\geq 6n + 7(k-3) + \frac{2(k-3)^2}{n} - 3n - 3k + 7$$

$$= 3n + 4k - 14 + \frac{2(k-3)^2}{n} \tag{1}$$

where we have used Jensen's inequality in the first step. Since $k \geq 0$, inequality (1) yields at least $3n - O(1)$ star-shaped polygons.

Our best lower bound construction is a *fan triangulation*, with a vertex of degree $n - 1$, shown in Figure 10 (right); it admits $\binom{n-1}{2}$ star-shaped polygons.

4.3 Directed paths

In a directed triangulation, every edge is a directed path of length 1, and the boundary of every triangular face contains at least one path of length two (that can be uniquely assigned to it). Since every triangulation on n points has at least $2n - 3$ edges and at least $n - 2$ triangular faces, it follows that every directed triangulation has at least $3n - 5$ directed paths of length 1 or 2. This bound is the best possible. Indeed, the directed triangulation shown in Figure 11 has $3n - 5$ directed paths: the $n - 1$ fan edges are directed upward and the remaining edges on the convex hull are directed clockwise or counterclockwise, in an alternating fashion. There are $2n - 3$ paths of length 1, and $n - 2$ paths of length 2, each lying on the boundary of a triangular face, and there are no paths of length 3 or higher.
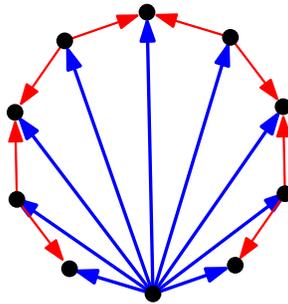

Figure 11: There are $\Theta(n)$ directed paths in this directed planar triangulation.

4.4 Monotone paths

4.4.1 Lower bound

We first argue that every triangulation contains $\Omega(n^2)$ monotone paths, since there is a monotone path connecting any pair of vertices. Indeed, this is a corollary of the following lemma applied to triangulations:

Lemma 6. [6][Lemma 1] *Let v be a vertex in a plane graph $G = (V, E)$ where every bounded face with $k \geq 3$ vertices is a convex k-gon, and the outer face is the exterior of the convex hull of V. Then G contains a spanning tree rooted at v such that all paths starting at v are monotone.*

It is also worth noting that the monotone path connecting a pair of vertices, u and v, is not necessarily monotone in the direction $\overrightarrow{uv}$. Also, two vertices are not always connected by an x-monotone path: a trivial lower bound for the number x-monotone paths is $\Omega(n)$, since every nonvertical edge is x-monotone. The triangulation $P_2 * P_{n-2}$ in Figure 10 (left) is embedded such that the path P_{n-2} is x-monotone and lies to the right of P_2. With this embedding, it contains $\Theta(n^2)$ x-monotone paths: every x-monotone path consists of a sequence of consecutive vertices of P_{n-2}, and 0, 1, or 2 vertices of P_2. However, both triangulations in Figure 10 admit $\Theta(n^4)$ monotone paths (over all directions).

Triangulations with a polynomial number of monotone paths are also provided by known constructions in which all monotone paths are "short". Dumitrescu, Rote, and Tóth [6] constructed triangulations with maximum degree $O(\log n / \log \log n)$ such that every monotone path has $O(\log n / \log n \log n)$ edges. Moreover, there exist triangulations with bounded vertex-degree in which every monotone path has $O(\log n)$ edges. These constructions contain polynomially many, but $\omega(n^4)$, monotone paths.

4.4.2 Upper bound

We construct a triangulation T of n points containing $O(n^{2\log 3} \log^2 n) = O(n^{3.17})$ monotone paths[1]. A similar construction was introduced in [6] as a stacked polytope in $\mathbb{R}^3$, where every monotone path on its 1-skeleton has $O(\log n)$ edges.

Theorem 3. *For every $n \in \mathbb{N}$, there is an n-vertex triangulation that contains $O(n^{2\log 3} \log^2 n) = O(n^{3.17})$ monotone paths.*

Construction. For every integer $\ell \geq 0$, we define a triangulation T on $n = 2^\ell + 2$ vertices. Refer to Figure 12. The outer face is a right triangle Δoab, where o is the origin and $\angle boa = \frac{\pi}{2}$. The interior vertices are arranged on ℓ circles, $C_0, C_1, \ldots, C_{\ell-1}$, centered at the origin, with the radii of the circles rapidly approaching 0. We place 2^i points on C_i, in an equiangular fashion, as described below, and so the number of interior points is $\sum_{i=0}^{\ell-1} 2^i = 2^\ell - 1$.

The rays to the points on C_i are interspersed with the rays to points on all previous layers. Specifically, the 2^i points on circle C_i are incident to rays emitted from the origin in directions $\frac{\pi}{4} + \frac{2j-1}{4 \cdot 2^i}\pi$ for $j = 1, \ldots, 2^i$. The edges of the triangulation are defined as follows. The origin o is connected to all other vertices. Each vertex on circle i is connected to the two vertices of the previous layers that are closest in angular order. The radii of the circles C_i are chosen recursively for $i = 0, 1, \ldots, \ell-1$, such that the edges that connect a vertex $v \in C_i$ to vertices v' and v'' on larger circles are almost parallel to ov' and ov'', respectively. Specifically, we require that $\angle vv'o < \pi/2^{\ell+1}$ and $\angle vv''o < \pi/2^{\ell+1}$ (so these angles are less than the angle between any two consecutive edges incident to o).

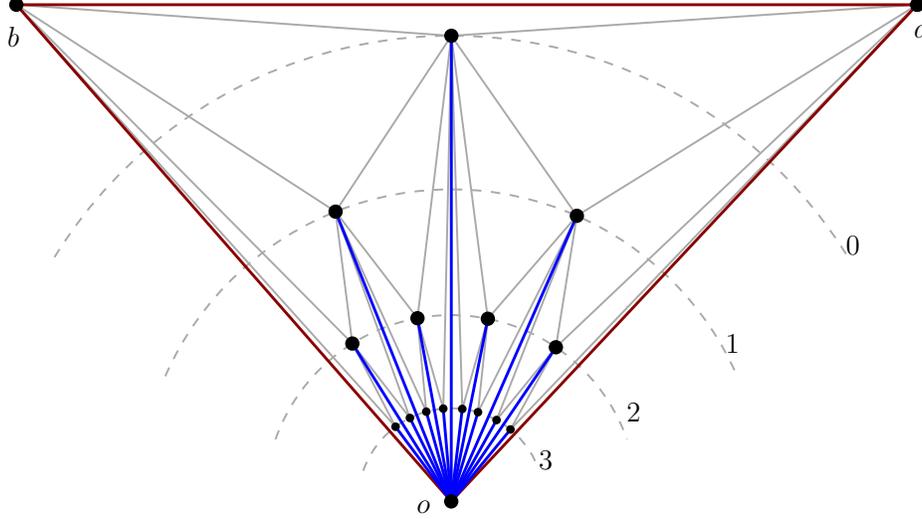---

[1]Throughout this paper, all logarithms are in base 2.

Figure 12: A schematic illustration of the triangulation T. The radii of the circles C_i, $i = 0, 1, \ldots, \ell - 1$, converge to 0 much faster than indicated in the figure.

Maximal monotone paths. In the argument, we sometimes focus on monotone paths that are *maximal* (with respect to containment). This is justified by the following easy lemma.

Lemma 7. *Let T be a triangulation of a point set S in the plane.*

(i) *The two endpoints of a maximal monotone path in T are vertices of the convex hull $\mathrm{conv}(S)$.*

(ii) *If T contains m maximal monotone paths, and every such path has at most k vertices, then the total number of monotone paths in T is at most $m\binom{k}{2}$.*

Proof. (i) Let $\xi = (v_1, \ldots, v_t)$ be a maximal path in T that is monotone in direction $\mathbf{u} \in \mathbb{R}^2 \setminus \{\mathbf{0}\}$. Suppose that the endpoint v_t lies in the interior of $\mathrm{conv}(S)$. Note that the angle between any two consecutive edges of T incident to an interior point of $\mathrm{conv}(S)$, to v_t in particular, is less than π, since each angle is an interior angle of a triangle. Consequently, there is an edge $v_t w$ in T such that $\langle \overrightarrow{v_t w}, \mathbf{u} \rangle > 0$. Now the path $(v_1, \ldots, v_t, w)$ is monotone in direction $\mathbf{u}$, and strictly contains ξ, in contradiction with the maximality of ξ.

(ii) Every subpath of a monotone path is also monotone (in the same direction). A path with $t \geq 2$ vertices has exactly $\binom{t}{2}$ subpaths, each determined by the two endpoints, and so the claim follows. $\square$

Analysis. We say that a (directed) edge or a path is *upward* if it is $(0, 1)$-monotone, and *downward* if it is $(0, -1)$-monotone. (The horizontal edge ab is neither upward nor downward). Clearly, every upward path is monotone in direction $(0, 1)$, but a path that contains both upward and downward edges may be monotone in some other direction $\mathbf{u} \in \mathbb{R}^2 \setminus \{\mathbf{0}\}$. Since o is the point with the minimum y-coordinate in T, every maximal upward path starts from o and ends at a or b. Consequently every upward path has at most one vertex on each circle, thus at most $\ell + 2 = O(\log n)$ vertices overall. In the remainder of the analysis, we bound the number of upward paths in T, and then show that every monotone path is composed of a small number (bounded by a constant) of upward and downward subpaths.

Lemma 8. *The number of maximal upward paths in T is $O(n^{\log 3})$. The number of upward paths is $O(n^{\log 3} \log n) = O(n^{1.585})$.*

Proof. Let τ_i denote the total number of upward paths that start from a point on the circle C_i and end at a or b. Observe that $\tau_0 = 2$ and $\tau_1 = 3 + 3 = 6$. Recall that by construction, each vertex on C_i is connected to the two vertices of the previous layers that are closest in angular order (left and right). It follows that

$$\tau_i = 2\sum_{j=0}^{i-1} \tau_j + 2, \text{ for } i \geq 1, \tag{2}$$

where the term 2 counts the direct edges to a and b from the leftmost and the rightmost points of C_i, respectively.

We now prove that $\tau_i = 2 \cdot 3^i$ for $i = 0, 1, \ldots, \ell - 1$. We proceed by induction on i. The base case $i = 0$ is satisfied as verified above by the value $\tau_0 = 2$. For the induction step, assume that the formula holds up to i. According to (2) we have

$$\tau_{i+1} = 2\sum_{j=0}^{i} \tau_j + 2 = 2\left(2\sum_{j=0}^{i} 3^j\right) + 2 = 2 \cdot 2 \cdot \frac{3^{i+1} - 1}{2} + 2 = 2 \cdot 3^{i+1} - 2 + 2 = 2 \cdot 3^{i+1},$$

as required. Write $\tau = \sum_{i=0}^{\ell-1} \tau_i$. Recall that $n = 2^\ell + 2$, hence

$$\tau = \sum_{i=0}^{\ell-1} \tau_i \leq 3^\ell \leq 3^{\log n} = n^{\log 3}. \tag{3}$$

It follows that the number of upward paths starting from vertices on $\bigcup_{i=0}^{\ell-1} C_i$ and ending at a or b is τ, and further, that the number of upward paths from o or $\bigcup_{i=0}^{\ell-1} C_i$ to a or b is 2τ. Since every such path has at most $\ell + 2$ vertices, the total number of upward paths is at most $(\ell + 1)\tau = O(n^{\log 3} \log n)$. $\qquad\square$

Corollary 1. *The number of upward paths in T starting from o is $O(n^{\log 3}) = O(n^{1.585})$.*

Proof. Let v_0 be a vertex on C_i, incident to two upward edges (v_0, v_1) and (v_0, v_2). Then all upward paths from o to v_0 lie in the union of two triangles $\Delta ov_0v_1 \cup \Delta ov_0v_2$. The subgraph of T lying in (the interior or on the boundary of) each of these triangles is isomorphic to the analogue of T on $2^{\ell-i} + 2$ vertices, with the same upward-downward orientations. As shown in the proof of Lemma 8, there are $O(3^{\ell-i})$ upward paths from o to v_0 in each of the triangles Δov_0v_1 and Δov_0v_2, and so T contains $O(3^{\ell-i})$ upward paths from o to v_0. Summing over all vertices of T, the total number of upward paths starting from o is

$$O\left(\sum_{i=0}^{\ell-1} 2^i \cdot 3^{\ell-i}\right) = O\left(3^\ell \sum_{i=0}^{\ell-1} \left(\frac{2}{3}\right)^i\right) = O\left(3^\ell\right) = O\left(3^{\log n}\right) = O\left(n^{\log 3}\right),$$

as claimed. $\qquad\square$

Lemma 8 also yields the following.

Corollary 2. *The number of monotone paths in T composed of one upward path and one downward path is $O(n^{2\log 3} \log^2 n) = O(n^{3.17})$.*

It remains to consider monotone paths in T that cannot be decomposed into one upward path and one downward path.[2] Every such path changes vertical direction (upward vs downward) at least twice.

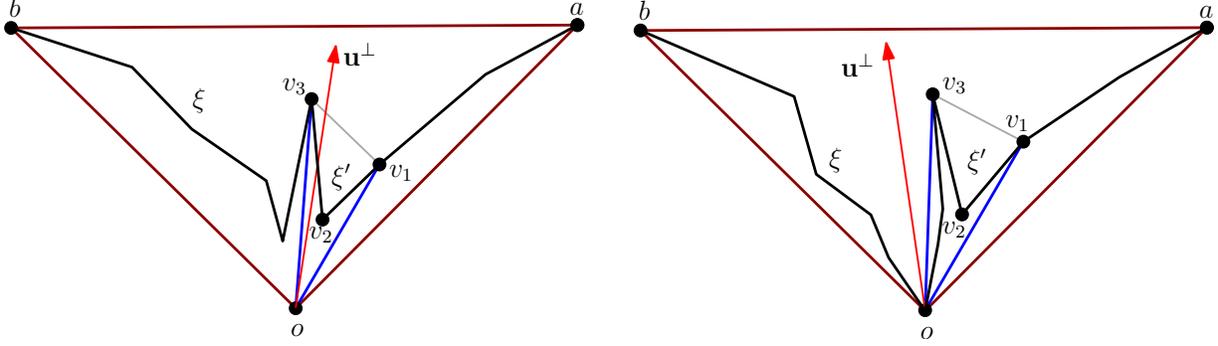[2]Such paths were inadvertently overlooked in the analysis from [14].

Figure 13: Two schematic pictures of a subpath $\xi' = (v_1, v_2, v_3)$ in T such that the edge (v_1, v_2) is downward, the edge (v_2, v_3) is upward, and $v_2 \neq o$. Left: A maximal monotone path ξ containing ξ', where $\xi \setminus \xi'$ lies in the exterior of Δov_1v_3. Right: A maximal monotone path ξ containing ξ', where part of $\xi \setminus \xi'$ lies inside Δov_1v_3.

Lemma 9. *The total number of monotone paths in T that change vertical direction at least twice is $O(n^{2\log 3} \log^2 n) = O(n^{3.17})$.*

Proof. We first characterize the monotone paths that change vertical direction at least twice, showing that in fact they change vertical direction at most three times; we then derive an upper bound on their number.

Let ξ be a maximal monotone path in T that changes vertical direction at least twice. Refer to Figure 13. By Lemma 7(i), the endpoints of ξ are vertices of the outer face Δoab. One of the endpoints of ξ is a or b, where all upward edges point to a or b, respectively. Consequently, ξ changes vertical directions at a vertex in the interior of Δoab from downward to upward. That is, ξ contains a subpath $\xi' = (v_1, v_2, v_3)$ such that (v_1, v_2) is downward, (v_2, v_3) is upward, and $v_2 \neq o$. By symmetry, we can assume that v_1 and v_3 are on the right and left sides of the ray $\overrightarrow{ov_2}$, respectively. By construction, v_1v_3, ov_1, and ov_3 are edges of T, so Δov_1v_3 is a 3-cycle in T.

Since both $\overrightarrow{v_1v_2}$ and $\overrightarrow{v_2v_3}$ are **u**-monotone, for some vector $\mathbf{u} \neq \mathbf{0}$, the orthogonal vector $\mathbf{u}^\perp$ lies between the directions of $\overrightarrow{v_2v_1}$ and $\overrightarrow{v_2v_3}$. By construction, these directions are within $\pi/2^{\ell+1}$ from the directions of $\overrightarrow{ov_1}$ and $\overrightarrow{ov_3}$, respectively. For every such vector $\mathbf{u}$, vertex a is **u**-minimal and b is **u**-maximal, and so ξ is a path from a to b.

The edges of ξ directly preceding and following $\xi' = (v_1, v_2, v_3)$ have a crucial role in determining the edges in $\xi \setminus \xi'$. The proof of Lemma 9 relies on the following two claims.

Claim 1. *If ξ does not change vertical direction at v_1, then v_1 uniquely determines the part of ξ preceding v_1. Similarly, if ξ does not change vertical direction at v_3, then v_3 uniquely determines the part of ξ following v_3.*

Proof. By symmetry, it is enough to prove the second statement. If $v_3 = b$, the proof is complete. Assume that $v_3 \neq b$, and label the portion of ξ starting at v_3 by $(v_3, v_4, \ldots, v_t)$. Recall that by construction, from every interior vertex v, there are two upward edges lying on opposite sides of the ray $\overrightarrow{ov}$.

We show by induction on $j = 3, \ldots, t$ that the edge (v_j, v_{j+1}) is upward, it lies on the left of $\overrightarrow{ov_j}$, and the other upward edge starting from v_j is incident to a vertex on or to the right of $\overrightarrow{ov_1}$. In the base case, $j = 3$, and by assumption (v_3, v_4) is upward. The upward edge on the right side of $\overrightarrow{ov_3}$ cannot enter the interior of Δov_1v_3 and so it must go to a vertex on or to the right of $\overrightarrow{ov_1}$. Thus this edge is not **u**-monotone, and so (v_3, v_4) must be the upward edge that leaves v_3 on the left side of $\overrightarrow{ov_3}$.

15

Assume now $3 < j < t$ and the induction hypothesis holds for v_{j-1}. By construction, the downward edges staring from v_j are almost parallel to $\overrightarrow{v_j o}$, and so they are not $\mathbf{u}$-monotone. By induction, an upward edge (v_{j-1}, r) is incident to a vertex on or to the right of $\overrightarrow{ov_1}$. Since the two upward edges (v_{j-1}, v_j) and (v_{j-1}, r) are incident to the same triangle of T, it follows that (v_j, r) is an edge in T. Hence, the upward edge on the right side of $\overrightarrow{ov_j}$ also goes to a vertex on or to the right of $\overrightarrow{ov_1}$, and so it is not $\mathbf{u}$-monotone. Consequently, the $\mathbf{u}$-monotone path ξ leaves v_j on the unique upward edge on the left side of $\overrightarrow{ov_j}$. $\qquad\square$

Claim 2. *If ξ arrives at v_1 on an upward edge, then $v_3 = b$ or ξ leaves v_3 on an upward edge. Similarly, if ξ leaves v_3 on a downward edge, then $v_1 = a$ or ξ arrives at v_1 on a downward edge.*

Proof. By symmetry, it is enough to prove the second statement. Assume that ξ leaves v_3 on a downward edge (v_3, v_4). Then the directions of (v_3, v_4) and (v_3, v_2) are both within $\pi/2^{\ell+1}$ from $\overrightarrow{v_3 o}$. Thus $\mathbf{u}^\perp$ is within $\pi/2^{\ell+1}$ from $\overrightarrow{ov_3}$. This, in turn, implies that none of the upward edges going into v_1 is $\mathbf{u}$-monotone, and the claim follows. $\qquad\square$

We continue with the proof of Lemma 9. If the path ξ changes vertical direction at neither v_1 nor v_3, then Claim 1 implies that ξ is composed of one upward path and one downward path, contradicting our assumption that ξ has no such decomposition.

Assume that the path ξ changes vertical direction at v_1 or v_3. Without loss of generality, assume that ξ changes vertical direction at v_3, i.e., ξ leaves v_3 on a downward edge. By Claims 1 and 2, the part of ξ preceding v_1 is uniquely determined. Note also that $\mathbf{u}^\perp$ is within $\pi/2^{\ell+1}$ from $\overrightarrow{ov_3}$.

We distinguish two cases based on whether the edge (v_3, v_4) of ξ following v_3 lies in the exterior of the triangle $\Delta ov_1 v_3$ or in its interior; then we estimate the number of such maximal paths ξ and their subpaths.

Case 1: v_4 lies in the exterior of $\Delta ov_1 v_3$; refer to Figure 13 (left). Then the vertices of ξ following v_4 are uniquely determined, analogously to Claim 1. We have $O(n)$ choices for v_2 (which determines the triple (v_1, v_2, v_3)), and $O(\log n)$ choices for v_4. Consequently, T contains $O(n \log n)$ maximal monotone paths ξ of this type. The length of any such path is $O(\log n)$, and by Lemma 7(ii), the total number of monotone paths of this type is $O(n \log^3 n)$.

Case 2: $v_4 = o$ or v_4 lies in the interior of $\Delta ov_1 v_3$; refer to Figure 13 (right). Then the path ξ reaches the $\mathbf{u}$-maximal vertex of $\Delta ov_1 v_3$, namely o. The portion of ξ inside $\Delta ov_1 v_3$ is a downward path from v_3 to o. The portion of ξ from o to b must be an upward path. In summary, the maximal monotone path ξ is composed of four upward or downward paths: A downward path from a to v_2, an upward edge (v_2, v_3), a downward path from v_3 to o, and an upward path from o to b.

Let us count the number of maximal monotone paths ξ of this type. By Lemma 8, there are $O(n^{\log 3})$ choices for the portion of ξ from o to b, and $O(n^{\log 3})$ independent choices for the portion from v_3 to o. Since the degree of v_3 is $O(\log n)$, we have $O(\log n)$ choices for vertex v_2. Finally, the portion from a to v_2 is uniquely determined by v_2 by Claim 1. This gives an $O(n^{2\log 3} \log n)$ bound on the number of maximal monotone paths of this type. The length of any such path is $O(\log n)$.

By Lemma 7(ii), the total number of monotone paths of this type is $O(n^{2\log 3} \log^3 n)$. By counting the subpaths of the maximal monotone paths ξ directly, we can reduce this bound by a logarithmic factor. If a subpath of ξ changes vertical directions twice, then its two endpoints must lie in the first and last portion of ξ, respectively. By Corollary 1, there are $O(n^{\log 3})$ choices for the portion of ξ from o to b *and* for all subpaths of ξ incident to o. The length of this last portion is $O(\log n)$, and so the number of its subpaths incident to v_2 is $O(\log n)$. Consequently, the total number of monotone paths of this type is $O(n^{2\log 3} \log^2 n)$.

Summing over both cases, it follows that the number of monotone paths that change vertical directions at least twice is $O(n^{2\log 3}\log^2 n)$, as claimed. $\qquad\square$

Proof of Theorem 3. The triangulation T contains $O(n^{\log 3}\log n)$ upward paths by Lemma 8, and $O(n^{2\log 3}\log^2 n)$ paths composed of one upward and one downward piece by Corollary 2. Any other monotone path $\xi = (v_1, \ldots, v_t)$ changes vertical direction (upward vs downward) at least twice. By Lemma 9, T contains $O(n^{2\log 3}\log^2 n)$ such paths. Consequently, the total number of monotone paths in T is $O(n^{2\log 3}\log^2 n) = O(n^{3.17})$, as claimed. $\qquad\square$

5   Conclusion

We have derived estimates on the maximum and minimum number of star-shaped polygons, monotone paths, and directed paths that a (possibly directed) triangulation of n points in the plane can have. Our results are summarized in Tables 1 and 2 of Section 1. Closing or narrowing the gaps between the upper and lower bounds remain as interesting open problems. The gaps in the last row of Table 1 and 2nd row of Table 2 are particularly intriguing.

Acknowledgments

References

[1] O. Aichholzer, T. Hackl, B. Vogtenhuber, C. Huemer, F. Hurtado, and H. Krasser, On the number of plane geometric graphs, *Graphs and Combinatorics* **23(1)** (2007), 67–84.

[2] M. Ajtai, V. Chvátal, M. Newborn, and E. Szemerédi, Crossing-free subgraphs, *Annals Discrete Math.* **12** (1982), 9–12.

[3] M. de Berg, O. Cheong, M. van Kreveld, and M. Overmars, *Computational Geometry: Algorithms and Applications*, 3rd edition, Springer, 2008.

[4] K. Buchin, C. Knauer, K. Kriegel, A. Schulz, and R. Seidel, On the number of cycles in planar graphs, in *Proc. 13th Annual International Conference on Computing and Combinatorics (COCOON)*, LNCS 4598, Springer, 2007, pp. 97–107.

[5] K. Buchin and A. Schulz, On the number of spanning trees a planar graph can have, in *Proc. 18th Annual European Symposium on Algorithms (ESA)*, LNCS 6346, Springer, 2010, pp. 110–121.

[6] A. Dumitrescu, G. Rote, and Cs. D. Tóth, Monotone paths in planar convex subdivisions, in *Discrete Geometry and Optimization (K. Bezdek, A. Deza, and Y. Ye, editors)*, vol. 69 of *Fields Institute Communications*, Springer, 2013, pp. 79–104.

[7] A. Dumitrescu, A. Schulz, A. Sheffer, and Cs. D. Tóth, Bounds on the maximum multiplicity of some common geometric graphs, *SIAM J. on Discrete Mathematics* **27(2)** (2013), 802–826.

[8] A. Dumitrescu and Cs. D. Tóth, Computational Geometry Column 54, *SIGACT News Bulletin* **43(4)** (2012), 90–97.

[9] A. Dumitrescu and Cs. D. Tóth, Convex polygons in geometric triangulations, in *Proc. 14th International Symposium on Algorithms and Data Structures (WADS)*, LNCS 9214, Springer, 2015, pp. 289–300.

[10] M. Hoffmann, A. Schulz, M. Sharir, A. Sheffer, C. D. Tóth, and E. Welzl, Counting plane graphs: flippability and its applications, in *Thirty Essays on Geometric Graph Theory (J. Pach, editor)*, Springer, 2013, pp. 303–326.

[11] R. A. Horn and C. R. Johnson, *Matrix Analysis*, Cambridge University Press, 1985.

[12] F. Hurtado, M. Noy, and J. Urrutia, Flipping edges in triangulations, *Discrete & Computational Geometry* **22(3)** (1999), 333–346.

[13] M. van Kreveld, M. Löffler, and J. Pach, How many potatoes are in a mesh?, in *Proc. 23rd International Symposium on Algorithms and Computation* (ISAAC), LNCS 7676, Springer, 2012, pp. 166–176.

[14] M. Löffler, A. Schulz, and Cs. D. Tóth, Counting carambolas, in *Proc. 25th Canadian Conference on Computational Geometry* (CCCG), Waterloo, ON, 2013, pp. 163–168.

[15] J. Pach and G. Tóth, Monotone drawings of planar graphs, *J. Graph Theory* **46(1)** (2004), 39–47.

[16] M. Sharir, A. Sheffer, and E. Welzl, Counting plane graphs: perfect matchings, spanning cycles, and Kasteleyn's technique, *J. Combin. Theory, Ser. A* **120(4)** (2013), 777–794.